

GSI Annual Report 2011 (extracts)

TASCA

Upgrade of the Gas-filled Recoil Separator TASCA and First Search Experiment for the New Element 120 in the Reaction $^{50}\text{Ti} + ^{249}\text{Cf}$ **Page 2**

C. E. Düllmann, A. Yakushev, J. Khuyagbaatar, D. Rudolph, H. Nitsche, D. Ackermann, L.-L. Andersson, M. Block, D. M. Cox, J. Dvorak, K. Eberhardt, P. A. Ellison, N. E. Esker, J. Even, C. Fahlander, U. Forsberg, J. M. Gates, K. E. Gregorich, P. Golubev, O. Gothe, W. Hartmann, R.-D. Herzberg, F. P. Heßberger, J. Hoffmann, R. Hollinger, A. Hübner, E. Jäger, J. Jeppsson, B. Kindler, S. Klein, I. Kojouharov, J. V. Kratz, J. Krier, N. Kurz, S. Lahiri, B. Lommel, M. Maiti, R. R. Mändl, S. Minami, A. Mistry, C. Mokry, J. P. Omtvedt, G. K. Pang, I. Pysmenetska, D. Renisch, J. Runke, L. G. Sarmiento, M. Schädel, B. Schausten, A. Semchenkov, J. Steiner, P. Thörle-Pospiech, N. Trautmann, A. Türler, J. Uusitalo, D. Ward, N. Wiehl, M. Wegrzecki, V. Yakusheva

Preparations towards X-Ray Fingerprinting of Element 115 Decay Chains **Page 3**

U. Forsberg, P. Golubev, L. G. Sarmiento, J. Jeppsson, D. Rudolph, L.-L. Andersson, D. Ackermann, M. Asai, M. Block, K. Eberhardt, J. Even, C. E. Düllmann, J. Dvorak, J. M. Gates, K. E. Gregorich, R.-D. Herzberg, F. P. Heßberger, E. Jäger, J. Khuyagbaatar, I. Kojouharov, J. V. Kratz, J. Krier, N. Kurz, S. Lahiri, B. Lommel, M. Maiti, E. Merchan, J. P. Omtvedt, E. Parr, J. Runke, H. Schaffner, M. Schädel, A. Yakushev

Search for short-lived uranium isotopes around N=126 **Page 4**

J. Khuyagbaatar, C. M. Mrosek, A. Yakushev, D. Ackermann, L.-L. Andersson, M. Block, D. M. Cox, C. E. Düllmann, J. Dvorak, K. Eberhardt, P. A. Ellison, N. E. Esker, J. Even, C. Fahlander, U. Forsberg, J. M. Gates, K. E. Gregorich, P. Golubev, O. Gothe, W. Hartmann, R.-D. Herzberg, F. P. Heßberger, J. Hoffmann, R. Hollinger, A. Hübner, E. Jäger, J. Jeppsson, B. Kindler, S. Klein, I. Kojouharov, J. V. Kratz, J. Krier, N. Kurz, S. Lahiri, B. Lommel, M. Maiti, R. R. Mändl, S. Minami, A. Mistry, C. Mokry, H. Nitsche, J. P. Omtvedt, G. K. Pang, I. Pysmenetska, D. Renisch, D. Rudolph, J. Runke, L. G. Sarmiento, M. Schädel, B. Schausten, A. Semchenkov, J. Steiner, P. Thörle-Pospiech, N. Trautmann, A. Türler, J. Uusitalo, D. Ward, N. Wiehl, M. Wegrzecki, V. Yakusheva

Metal carbonyl complexes - a new compound class accessible for transactinides **Page 5**

J. Even, A. Yakushev, C. E. Düllmann, J. Dvorak, R. Eichler, O. Gothe, D. Hild, E. Jäger, J. Khuyagbaatar, J. V. Kratz, J. Krier, L. Niewisch, H. Nitsche, I. Pysmenetska, M. Schädel, B. Schausten, A. Türler, N. Wiehl, D. Wittwer

Preparation of ^{249}Cf targets from pre-used material **Page 6**

J. Runke, C. E. Düllmann, K. Eberhardt, P. A. Ellison, K. E. Gregorich, E. Jäger, B. Kindler, J. Krier, B. Lommel, C. Mokry, H. Nitsche, M. Schädel, P. Thörle-Pospiech, N. Trautmann, A. Yakushev

Background Reduction in TASCA **Page 7**

J. M. Gates, K. E. Gregorich, L.-L. Andersson, C. E. Düllmann, J. Dvorak, J. Even, K. Eberhardt, U. Forsberg, D. Hild, E. Jäger, J. Jeppsson, J. Khuyagbaatar, J. V. Kratz, J. Krier, J. P. Omtvedt, I. Pysmenetska, D. Renisch, D. Rudolph, M. Schädel, A. Semchenkov, A. Vascon, N. Wiehl, A. Yakushev

IRiS

IRiS - Feasibility Calculations **Page 8**

J. Dvorak, C. E. Düllmann

Theory

Theoretical Predictions of Properties of Element 119 and its Adsorption on Noble Metal Surfaces

V. Pershina, A. Borschevsky, J. Anton **Page 9**

Prediction of Atomic Properties of Ra and Element 120 **Page 10**

A. Borschevsky, V. Pershina, E. Eliav, U. Kaldor

Theoretical Studies on Formation and Adsorption of MBr_5 and MOBr_3 ($\text{M} = \text{Nb}, \text{Ta}, \text{and Db}$) on KCl/KBr Surfaces **Page 11**

J. Anton, V. Pershina

Upgrade of the Gas-filled Recoil Separator TASCAs and First Search Experiment for the New Element 120 in the Reaction $^{50}\text{Ti} + ^{249}\text{Cf}$

Ch.E. Düllmann^{1,2,3}, A. Yakushev², J. Khuyagbaatar^{2,3}, D. Rudolph⁴, H. Nitsche⁵, D. Ackermann², L.-L. Andersson^{3,6}, M. Block², D.M. Cox⁶, J. Dvorak³, K. Eberhardt¹, P.A. Ellison⁵, N.E. Esker⁵, J. Even^{1,3}, C. Fahlander⁴, U. Forsberg⁴, J.M. Gates⁵, K.E. Gregorich⁵, P. Golubev⁴, O. Gothe⁵, W. Hartmann², R.-D. Herzberg⁶, F.P. Heßberger^{2,3}, J. Hoffmann², R. Hollinger², A. Hübner², E. Jäger², J. Jeppsson⁴, B. Kindler², S. Klein¹, I. Kojouharov², J.V. Kratz¹, J. Krier², N. Kurz², S. Lahiri⁷, B. Lommel², M. Maiti⁷, R.R. Mändl^{2,8}, S. Minami², A. Mistry⁶, C. Mokry¹, J.P. Omtvedt⁹, G.K. Pang⁵, I. Pysmenetska², D. Renisch¹, J. Runke², L.G. Sarmiento¹⁰, M. Schädel^{2,11}, B. Schausten², A. Semchenkov⁹, J. Steiner², P. Thörle-Pospiech¹, N. Trautmann¹, A. Türler¹², J. Uusitalo¹³, D. Ward⁴, N. Wiehl¹, M. Wegrzecki¹⁴, V. Yakusheva³

¹U. Mainz, Germany, ²GSI, Darmstadt, Germany, ³HIM, Mainz, Germany, ⁴Lund U, Sweden, ⁵LBNL+UC Berkeley, CA, USA, ⁶U. Liverpool, UK, ⁷SINP, Kolkata, India, ⁸FH Frankfurt, ⁹U. Oslo, Norway, ¹⁰UNAL Bogotá, Colombia, ¹¹JAEA Tokai, Japan, ¹²U. Bern+PSI Villigen, Switzerland ¹³U. Jyväskylä, Finland, ¹⁴ITE Warsaw, Poland

The heaviest elements were discovered in ^{48}Ca -induced fusion reactions with actinide targets [1]. The observation of the hitherto heaviest element 118 was claimed from irradiations of targets of ^{249}Cf , which is the highest-Z nucleus that is available in sufficient quantities. Hence, to search for elements beyond $Z=118$, reactions induced by projectiles with $Z>20$ are required. Previously, $^{64}\text{Ni}+^{238}\text{U}$ [2], $^{58}\text{Fe}+^{244}\text{Pu}$ [3], and recently $^{54}\text{Cr}+^{248}\text{Cm}$ [4] were studied, but element 120 is yet to be discovered. Theoretical predictions [5-8] agree on the $^{50}\text{Ti}+^{249}\text{Cf}$ reaction to have the highest cross section. Accordingly, the TASCAs collaboration selected this reaction to search for element 120. Maximum predicted cross sections range from 0.04 pb [5] to 0.75 pb [6, 8]. For comparison, the $^{48}\text{Ca}+^{249}\text{Cf} \rightarrow Z=118$ experimental cross section is $0.5_{-0.3}^{+1.6}$ pb [9].

On the way to a first search experiment for element 120 at TASCAs, upgrades of several key components were performed, compared to the setup as used for the $^{244}\text{Pu}(^{48}\text{Ca},3\text{-}4\text{n})^{288,289}\text{114}$ reaction [10, 11]. These include the implementation of a larger-area target wheel with 100 mm diameter comprising four targets [12]. The heat of each 5-ms long UNILAC macropulse is now dissipated over a four times larger area (6 cm^2) than in the old system (1.4 cm^2) used for element 114.

The separation from unwanted nuclear reaction products was increased by a factor of ~ 10 [13] by (i) implementing a carbon stripper foil in front of the target to increase the beam charge state, (ii) a fixed scraper mounted in the center of the first quadrupole magnet, and (iii) a second, moveable scraper mounted behind the second quadrupole. Both scraper positions were chosen based on ion-optical simulations, which predicted significant background suppression without loss in EVR efficiency due to the scrapers. Measurements, e.g., of the $^{48}\text{Ca}+^{208}\text{Pb}$ reaction, confirmed the expectations (see also [14]). The efficiency of TASCAs for element 120 produced in the reaction $^{50}\text{Ti}+^{249}\text{Cf}$ was calculated to be $(62\pm 6)\%$. Discrimination between various event types was enhanced by improving the multi-wire proportional counter veto detector

efficiency compared to the element 114 experiment. Several predictions of decay properties of isotopes produced in the $^{50}\text{Ti}+^{249}\text{Cf}$ reaction suggest their half-lives, $T_{1/2}$, to be on the order of μs . This is shorter than the dead-time of the data acquisition (DAQ) system used in 2009 [11]. Therefore, a fast digital sampling pulse processing system was built and integrated into the DAQ system [15]. This allowed registering events with $T_{1/2}$ as short as 100 ns, as confirmed in a study of the reaction $^{50}\text{Ti}+^{176}\text{Yb}$, which yields decay chains with very short-lived members [16].

Old ^{249}Cf samples were chemically reprocessed and electrodeposited on $\sim 2.2\text{-}\mu\text{m}$ thick Ti backings by molecular plating [17], yielding $\sim 0.5\text{-mg/cm}^2$ thick targets.

In August-October 2011, a first experiment to search for element 120 was conducted. Intense beams ($0.5\text{-}1.0\text{ }\mu\text{A}_{\text{part}}$) were applied on the Cf targets during 39 days of beamtime. The data analysis is in progress.

Acknowledgments: We thank the ion source and accelerator staff for providing stable and intense ^{50}Ti beams, and the experimental electronics department for making the digital DAQ system available on a short time-scale. Work supported by the Helmholtz Institute Mainz.

References

- [1] Y. Oganessian, *Radiochim. Acta* **99**, 429 (2011).
- [2] S. Hofmann *et al.*, *GSI Sci. Rep.* 2008 (2009) p. 131.
- [3] Yu.Ts. Oganessian *et al.*, *Phys. Rev. C* **79**, 024603 (2009).
- [4] S. Hofmann *et al.*, this Scientific Report (2012).
- [5] V. Zagrebaev *et al.*, *Phys. Rev. C* **78**, 034610 (2008).
- [6] G. G. Adamian *et al.*, *Eur. Phys. J. A* **41**, 235 (2009).
- [7] A. K. Nasirov *et al.*, *Phys. Rev. C* **84**, 044612 (2011).
- [8] K. Siwek-Wilczynska *et al.*, *IJMP* **19**, 500 (2010).
- [9] Yu.Ts. Oganessian *et al.*, *Phys. Rev. C* **74**, 044602 (2006).
- [10] Ch.E. Düllmann *et al.*, *Phys. Rev. Lett.* **104**, 252701 (2010).
- [11] J.M. Gates *et al.*, *Phys. Rev. C* **83**, 054618 (2011).
- [12] T. Torres *et al.*, *GSI Sci. Rep.* 2010 (2011) p. 236.
- [13] J. M. Gates *et al.*, this Scientific Report (2012).
- [14] U. Forsberg *et al.*, this Scientific Report (2012).
- [15] N. Kurz *et al.*, this Scientific Report (2012).
- [16] J. Khuyagbaatar *et al.*, this Scientific Report (2012).
- [17] J. Runke *et al.*, this Scientific Report (2012).

Preparations towards X-Ray Fingerprinting of Element 115 Decay Chains*

U. Forsberg¹, P. Golubev¹, L. G. Sarmiento², J. Jeppsson¹, D. Rudolph¹, L.-L. Andersson^{3,4}, D. Ackermann⁵, M. Asai⁶, M. Block⁵, K. Eberhardt⁷, J. Even^{4,7}, Ch. E. Düllmann^{4,5,7}, J. Dvorak⁴, J. M. Gates⁸, K. E. Gregorich⁸, R.-D. Herzberg³, F. P. Heßberger^{4,5}, E. Jäger⁵, J. Khuyagbaatar⁴, I. Kojouharov⁵, J. V. Kratz⁷, J. Krier⁵, N. Kurz⁵, S. Lahiri⁹, B. Lommel⁵, M. Maiti⁹, E. Merchán⁵, J. P. Omtvedt¹⁰, E. Parr³, J. Runke⁵, H. Schaffner⁵, M. Schädel^{5,6}, and A. Yakushev⁵

¹Lund University, Lund, Sweden; ²Universidad Nacional de Colombia, Bogotá, Colombia; ³University of Liverpool, Liverpool, United Kingdom; ⁴Helmholtz Institute Mainz, Mainz, Germany; ⁵GSI Helmholtzzentrum für Schwerionenforschung, Darmstadt, Germany; ⁶Advanced Science Research Center, Japan Atomic Energy Agency, Tokai, Japan; ⁷Johannes Gutenberg-Universität Mainz, Mainz, Germany; ⁸Lawrence Berkeley National Laboratory, Berkeley, USA; ⁹Saha Institute of Nuclear Physics, Kolkata, India; ¹⁰University of Oslo, Oslo, Norway

In preparation for an approved experiment aiming at X-ray fingerprinting of element 115 decay chains to unambiguously determine the atomic number of the involved nuclei, a number of final tests were performed in June 2011. The main experiment is designed to measure the energies of characteristic X-rays emitted following de-excitation via internal conversion in coincidence with α decays into excited states. $^{287}\text{115}$ will be produced in the $^{243}\text{Am}(^{48}\text{Ca},4n)$ reaction, isolated in the gas-filled recoil separator TASCA [1], and guided to the TASI-Spec setup [2].

In this experiment we studied which of the two ion-optical modes of TASCA [1] is more beneficial to use together with TASI-Spec. Previously, TASI-Spec has been used with TASCA in the “Small image mode” (SIM) with good results. However, simulations and experiments [4] have shown that insertion of slits inside TASCA can decrease the background in “High transmission mode” (HTM) significantly. To investigate the performance of TASI-Spec with TASCA in HTM, the reaction $^{208}\text{Pb}(^{48}\text{Ca},2n)^{254}\text{No}$ was used (for details, see [3]). First, the previously determined optimal TASCA SIM quadrupole magnet settings for TASI-Spec were confirmed to yield the maximum transmission. Secondly, a series of HTM tests using the nominal TASCA focal-plane detector confirmed that a strong background suppression can be achieved by inserting slits in TASCA. Thirdly, the HTM magnet settings were optimized to give the best transmission of ^{254}No into TASI-Spec. This optimization was guided by simulations [5] of the trajectories of ^{254}No through TASCA. Relative experimental transmissions were derived from the number of events recorded in the α peak from ^{254}No in the TASI-Spec implantation detector, normalized to the beam integral. The optimal settings were found within the range of magnet settings suggested by the simulations.

The spacial distribution of ^{254}No events over the TASI-Spec implantation detector with TASCA in HTM is illustrated in Fig. 1(b), showing data from a simulation of the

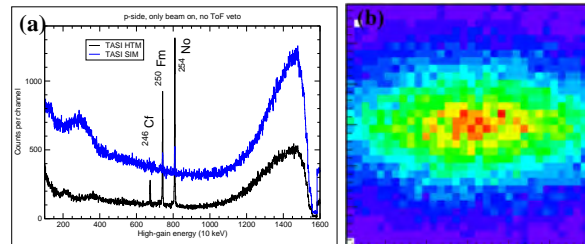


Figure 1: (a) Energy spectra accumulated using SIM (blue) and HTM (black). (b) Simulated distribution, in HTM, of ^{254}No in the TASI-Spec implantation detector [3].

experiment. The implantation profile is elongated in the horizontal direction, as expected in HTM. Since the ions have to pass a cylindrical tube on their way to TASI-Spec, the best use of the two focusing quadrupoles turned out to be when the horizontal focusing is somewhat stronger than the vertical one. The optimized settings established in this experiment can be used for determining how to tune the magnets in other experiments using TASI-Spec with HTM.

The transmission to TASI-Spec with TASCA in HTM was $\sim 80\%$ of the one achieved in SIM. The main advantage in HTM is the excellent background suppression. Fig. 1(a) shows beam-on energy spectra from SIM (blue) and HTM with slits inserted (black). The clean HTM spectrum implies that it is possible to search for α -X-ray coincidences in the beam-on periods as well as in the beam-off periods, even without using a veto detector, such as a MWPC, for implanted particles. In SIM, only beam-off data can be used when no MWPC is installed, due to too high background rates during beam-on periods. Since the beam-on data accounts for 25% of the events due to the duty cycle of the beam, the total amount of TASI-Spec data is comparable for HTM and SIM.

References

- [1] A. Semchenkov *et al.*, Nucl. Instr. Meth. **B266**, 4153 (2008)
- [2] L.-L. Andersson *et al.*, Nucl. Instr. Meth. **A622**, 164 (2010)
- [3] U. Forsberg *et al.*, Acta Phys. Pol. B, in press
- [4] J. M. Gates *et al.*, contribution to this report
- [5] K. E. Gregorich *et al.*, GSI Scientific Report, 144 (2006)

* This work was co-funded by the European Commission under the capacities program (Grant Agreement Number FP7-227867, ENSAR), and supported by the Helmholtz Institute Mainz. We also thank the Royal Physiographical Society in Lund for funding of equipment.

Search for short-lived uranium isotopes around N=126 *

J. Khuyagbaatar^{1,2}, Ch.M. Mrosek³, A. Yakushev¹, D. Ackermann¹, L.-L. Andersson^{2,4}, M. Block¹, D.M. Cox⁴, Ch.E. Düllmann^{1,2,3}, J. Dvorak², K. Eberhardt³, P.A. Ellison⁵, N.E. Esker⁵, J. Even^{2,3}, C. Fahlander⁶, U. Forsberg⁶, J.M. Gates⁵, K.E. Gregorich⁵, P. Golubev⁶, O. Gothe⁵, W. Hartmann¹, R.-D. Herzberg⁴, F.P. Heßberger^{1,2}, J. Hoffmann¹, R. Hollinger¹, A. Hübner¹, E. Jäger¹, J. Jeppsson⁶, B. Kindler¹, S. Klein³, I. Kojouharov¹, J.V. Kratz³, J. Krier¹, N. Kurz¹, S. Lahiri⁷, B. Lommel¹, M. Maiti⁷, R.R. Mändl^{1,8}, S. Minami¹, A. Mistry⁴, C. Mokry³, H. Nitsche⁵, J.P. Omtvedt⁹, G.K. Pang⁵, I. Pysmenetska¹, D. Renisch³, D. Rudolph⁶, J. Runke¹, L.G. Sarmiento¹⁰, M. Schädel^{1,11}, B. Schausten¹, A. Semchenkov⁹, J. Steiner¹, P. Thörle-Pospiech³, N. Trautmann³, A. Türler¹¹, J. Uusitalo¹³, D. Ward⁶, N. Wiehl³, M. Wegrzecki¹⁴, V. Yakusheva²

¹GSI, Darmstadt, Germany, ²HIM, Mainz, Germany, ³U. Mainz, Germany, ⁴U. Liverpool, UK, ⁵LBNL+UC Berkeley, CA, USA, ⁶Lund U. Sweden, ⁷SINP, Kolkata, India, ⁸FH Frankfurt, ⁹U. Oslo, Norway, ¹⁰UNAL Bogotá, Colombia, ¹¹JAEA Tokai, Japan, ¹²U. Bern+PSI Villigen, Switzerland ¹³U. Jyväskylä, Finland, ¹⁴ITE Warsaw, Poland,

Production and decay of short-lived ²²¹U (previously unknown) and ²²²U (only the half-life is known) were studied at the gas-filled separator TASCA. These two nuclei have only few neutrons more than the magic number N=126, which leads to high α decay Q-values and, therefore, to very short half-lives (< 10 μ s). To explore this microsecond/sub-microsecond half-life region, digital electronics was implemented into a combined “ANalog” and “DIgital” (ANDI) data acquisition system [1].

A ⁵⁰Ti¹²⁺ beam was accelerated to energies $E_{\text{lab}}=230$ and 240 MeV and irradiated a rotating ¹⁷⁶Yb target wheel to produce ²²²U and ²²¹U in 4n and 5n de-excitation channels of the complete fusion reaction, respectively.

The evaporation residues (ER) were separated from the primary beam by TASCA and implanted into the stop detector consisting of two double-sided silicon-strip detectors. Two signals, one from each side of the stop detector were processed in two different parts of the ANDI system with a common trigger and zero suppression [1]. The signals from 144 vertical front strips were processed by analog amplifiers connected to peak-sensing ADCs [2]. The preamplified signals from 48 horizontal back strips were processed by sampling ADC's (FEBEX2) with 60 MHz frequency. Traces with total length of 50 μ s (7 μ s before and 43 μ s after) were recorded following an accepted trigger. The deadtime of the “analog” part was shorter than 43 μ s. Therefore it was always ready to accept the next triggered event [1]. Further, both data were combined into single events by an event builder of MBS [1].

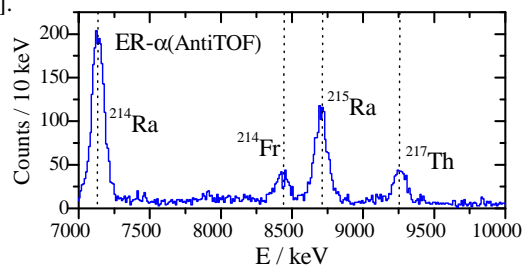


Fig 1: An energy spectrum of α -particles from the ER- α correlation up to 14 s, with both events occurring in the same pixel.

* Work supported by HI Mainz

An ER- α correlation analysis was performed to find recoiling nuclei and identify the measured α lines (Fig. 1). Only α -particle events were considered without a signal from the time-of-flight detector. Alpha decays of ²¹⁴Ra, ²¹⁵Ra, ²¹⁴Fr, and ²¹⁷Th were identified. From further analyses the decay of ²¹⁴Fr was found as a member of ER- α (7-18MeV)- α (²¹⁴Fr) chains. The second member of this chain is typically a pile-up of two α decays. These events were investigated using the data from the “digital” part. Clearly two signals were found in traces of them and α decays of ²²²Pa and ²¹⁸Ac were unambiguously determined (see Fig. 2a).

The traces of the ER's from ER- α (²¹⁴Ra) were investigated in order to find “missing” α decays of mother ²¹⁸Th and grandmother ²²²U nuclei. In most cases only single signals were found, pointing to the implantation of ²¹⁴Ra. However, traces with two and three signals were also found (see Fig. 2b). These data allow us to unambiguously assign α decays of ²¹⁸Th and ²²²U.

The traces of the ER's from ER- α (²¹⁷Th) were investigated to find the α decay of the new nucleus ²²¹U. In most cases a single ER signal was seen. However, traces with two signals, which include the α decay of the new nucleus ²²¹U, were also found (see Fig. 2c). More detailed information will be provided in [3].

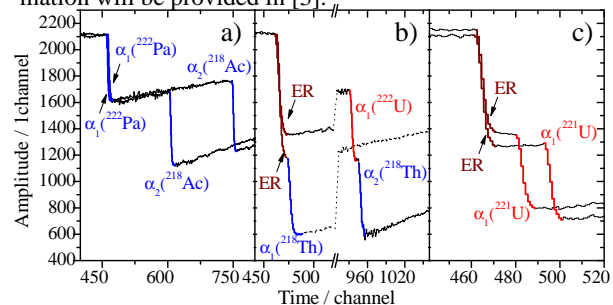


Fig 2: Example of traces of pile-up α -particles correlated with ²¹⁴Fr a), ER's correlated with ²¹⁴Ra b), and with ²¹⁷Th c).

[1] N. Kurz et al., this Scientific Report (2012).

[2] J.M. Gates et al., Phys. Rev. C. 83 054618 (2011).

[3] J. Khuyagbaatar et al., to be published.

Metal carbonyl complexes – a new compound class accessible for transactinides

J. Even^{1,2#}, A. Yakushev³, Ch.E. Düllmann^{1,2,3}, J. Dvorak², R. Eichler⁴, O. Gothe⁵, D.Hild¹, E. Jäger³, J. Khuyagbaatar^{2,3}, J.V. Kratz¹, J.Krier³, L. Niewisch¹, H. Nitsche⁵, I. Pysmenetska¹, M. Schädel^{3,7}, B. Schausten³, A. Türler^{4,6}, N. Wiehl¹, D. Wittwer^{4,6}

¹University Mainz, Mainz, Germany; ²HIM, Mainz, Germany; ³GSI, Darmstadt, Germany; ⁴PSI, Villigen, Switzerland, ⁵LBNL, Berkeley, CA, USA; ⁶University of Berne, Berne, Switzerland; ⁷JAEA, Tokai, Japan

Gas-phase chemical studies of transactinide elements were so far restricted to simple, thermally stable, inorganic compounds. Metal-carbonyl complexes would provide a link to metal-organic chemistry. Binary, mononuclear, volatile carbonyl complexes are known for all lighter elements of group 6 and 8 of the periodic table. Seaborgium hexacarbonyl has been predicted to be stable [1]. Its experimental study would be interesting, because relativistic effects are predicted to influence the metal-CO bond.

We explored the method of rapid in-situ synthesis of transition-metal carbonyl complexes with short-lived isotopes. First tests were performed at the TRIGA Mainz reactor, using the ²⁴⁹Cf(n,f) reaction. Recoiling fission products were thermalized either in pure N₂ or in a CO/N₂-mixture. All volatile compounds were transported in a gas stream to an activated charcoal trap, which was monitored with a γ -ray detector. Figure 1 shows a typical spectrum from the CO/N₂ measurements.

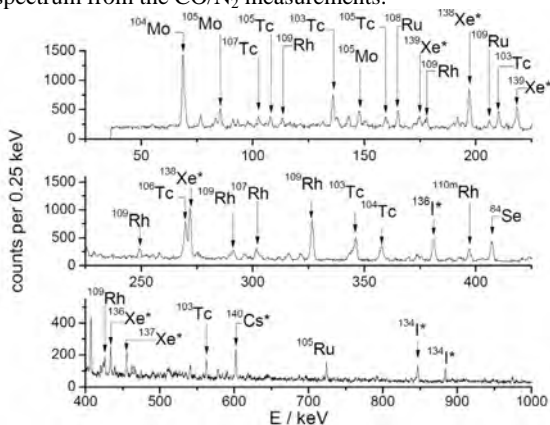


Figure 1: γ -ray spectrum of fission products transported in a CO/N₂ mixture collected for 2 min in a charcoal trap. Subsequently, the sample was measured for 2 min. γ -lines, which were also visible in spectra of pure N₂ experiments, are marked with *.

Short-lived isotopes of Se, Mo, Tc, Ru and Rh were only observed in the spectra when CO was added. These elements form volatile compound with the CO. Transport with cluster (aerosol) material can be excluded.

To test this method under experimental conditions relevant for transactinides, α -decaying ¹⁶³W, ¹⁶⁴W, ¹⁷⁰Os and ¹⁷¹Os were produced in ¹⁴⁴Sm(²⁴Mg,4-5n) and ¹⁵²Gd(²⁴Mg,4-5n) reactions at the gas-filled recoil separator TASCA. Evaporation residues were separated from the

* Work supported by the Helmholtz Institute Mainz, the Research Center Elementary Forces and Mathematical Foundations (EMG), the BMBF under contract No. 06MZ223I, and the Swiss National Science Foundation under contract No. 200020 126639 #evenj@uni-mainz.de

primary beam and from unwanted transfer products with TASCA. They were thermalized in mixtures of He and CO in a Recoil Transfer Chamber (RTC) [2] at the TASCA focal plane. Volatile carbonyl complexes – most likely Os(CO)₅ and W(CO)₆ – were formed in the RTC and were transported with the gas stream to the thermochromatography detector COMPACT [3]. The COMPACT detector array is a chromatography channel consisting of SiO₂ covered PIN diodes, suitable to register α particles emitted from volatile species inside the channel. A negative temperature gradient was applied along the chromatography column. Figure 2 shows thermochromatograms of Os(CO)₅ and W(CO)₆. The measurements are compared to Monte Carlo Simulations. From the deposition patterns of W and Os, adsorption enthalpies of W(CO)₆ of (-46.5 \pm 2.5) kJ/mol and (-43^{+3.5}_{-2.5}) kJ/mol for Os(CO)₅ were deduced. These values indicate physisorption of these carbonyl complexes on SiO₂.

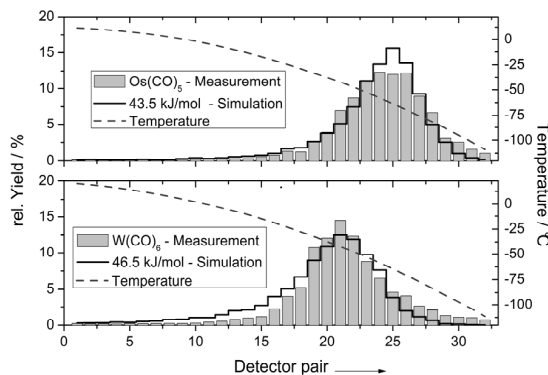


Figure 2: Upper graph: combined thermochromatogram of ¹⁷⁰Os(CO)₅ and ¹⁷¹Os(CO)₅. Lower graph: combined thermochromatogram of ¹⁶³W(CO)₆ and ¹⁶⁴W(CO)₆.

Based on the results of our experiments, Sg(CO)₆ and Hs(CO)₅ are now within reach for transactinide chemistry. These compounds are suitable for chemical characterization by thermochromatography and appear highly promising for nuclear spectroscopy under low background conditions.

References

- [1] C. S. Nash, B. E. Bursten, J. Am. Chem. Soc. **121** (1999) 10830.
- [2] J. Even et al., Nucl. Instr. Meth. A. **638**, (2011) 157.
- [3] J. Dvorak et al., Phys. Rev. Lett. **100** (2008) 132503.

Preparation of ^{249}Cf targets from pre-used material

J. Runke¹, Ch.E. Düllmann^{1,2,3}, K. Eberhardt², P.A. Ellison^{4,5}, K.E. Gregorich⁴, E. Jäger¹, B. Kindler¹, J. Krier¹, B. Lommel¹, C. Mokry², H. Nitsche^{4,5}, M. Schädel⁶, P. Thörle-Pospiech², N. Trautmann², A. Yakushev¹

¹GSI Helmholtzzentrum für Schwerionenforschung GmbH, Darmstadt, Germany; ²Johannes Gutenberg-Universität Mainz, Germany; ³Helmholtz-Institut Mainz, Germany; ⁴Lawrence Berkeley National Laboratory, Berkeley, CA, USA; ⁵University of California, Berkeley, CA, USA; ⁶Advanced Science Research Center, Japan Atomic Energy Agency, Tokai, Japan

For the synthesis of the new element with atomic number $Z = 120$, the fusion reaction of ^{50}Ti with ^{249}Cf was studied at the gas-filled recoil separator TASCA [1]. Pre-used ^{249}Cf , originating from the decay of ^{249}Bk , was provided by the Lawrence Berkeley National Laboratory to produce suitable targets.

The chemical form of the delivered ^{249}Cf was either the oxide, chloride or the nitrate. In a first step the material was dissolved in 8 M HCl. The ^{249}Cf solution contained Al, Fe, Pb and Ti as impurities. In a first purification step the anion-exchanger BioRad AG MP-1M was applied to remove Al and Fe from the solution. In the second step a cation exchange column with DOWEX 50WX8 was used for the removal of Pb and Ti. Over both purification steps the Cf recovery was almost 100 %.

A rotating target wheel assembly was used, which was previously tested to accept high beam intensities up to 2 μA (particle). Molecular plating (MP) [2] was employed for the preparation of ^{249}Cf layers on $\sim 2.2\text{-}\mu\text{m}$ thick Ti backing foils produced by cold rolling at GSI.

The average foil thickness was determined by weighing, whereas the homogeneity of the foil thickness was checked by α -particle energy-loss measurements over 5 positions per foil. The standard deviation of the foil thickness varied between 0.03 and 0.14 μm .

The deposition parameters for Cf were optimized in experiments with Gd. This also included MP with ^{153}Gd -tracer to verify the homogeneity of the Gd layer using a commercial radiographic imager [3] (FLA 7000 from FUJIFILM Corp.).

The first step in the MP of Cf was the conversion of the Cf chloride into the nitrate by evaporation to dryness and re-dissolution in 8 M HNO_3 . An aliquot of the Cf-solution with about 3 mg of ^{249}Cf (455 MBq) was evaporated to dryness in a TeflonTM beaker. The green residue was re-dissolved in a small volume (100 μl) of 0.1 M HNO_3 . The solution was transferred into an electrochemical deposition cell (EDC) made of PEEK. The beaker was washed with 3 x 300 μl isopropanol, which was also transferred to the EDC. The EDC was filled up to a volume of 52 ml with isobutanol. For the mixing during the deposition process an ultrasonic stirrer was used [3]. For the MP of ^{249}Cf with a surface of 6 cm^2 a voltage of 200 – 600 V at a maximum current density of about 0.3 mA/cm^2 was applied. The deposition time was 4 – 5 hours. The deposition yield exceeded 90 %. Fig. 1 shows one of the produced target segments.



Figure 1: Cf target-segment

Prior to the production of $\sim 0.5\text{-mg}/\text{cm}^2$ thick ^{249}Cf targets, a thin ^{249}Cf target was prepared. With this target we tested the deposition parameters. Before the deposition, and in 1-h steps during the MP process, 10 μl aliquots of the ^{249}Cf -solution were evaporated to dryness for α -particle spectroscopy. With these measurements the decreasing Cf content in the solution during the deposition was determined as well as the deposition yield.

As a method for the yield determination, γ spectroscopy was used. For this, the thin ^{249}Cf target served as a reference sample. The distance from the target to the γ detector was about 3 m, the dead time was 5%. The data confirmed a thickness of $\sim 0.5\text{-mg}/\text{cm}^2$, and the final analysis of the thickness values, including measurements performed after the element 120 experiment [1], is in progress.

Acknowledgments: We would like to thank Robert F. Fairchild II, Naomi E. Reeves, John A. van Wart and LBNL's entire Radiation Protection Group of the Environmental Health and Safety Division for their leadership and active support with the preparation and execution of the ^{249}Cf shipment to Germany. This work was supported by the Helmholtz Institute Mainz.

References

- [1] Ch.E. Düllmann et al., this scientific report (2012).
- [2] K. Eberhardt et al., Nucl. Instrum. Meth. Phys. Res. A590, 134 (2008).
- [3] A. Vascon et al., Nucl. Instrum. Meth. Phys. Res. A655, 72 (2011).

Background Reduction in TASCA

J.M Gates^{1,#}, K.E. Gregorich¹, L.-L. Andersson², Ch.E. Düllmann^{3,4,5}, J. Dvorak⁵, J. Even^{3,5}, K. Eberhardt³, U. Forsberg⁶, D. Hild³, E. Jäger⁴, J. Jeppsson⁶, J. Khuyagbaatar^{4,5}, J.V. Kratz³, J. Krier⁴, J.P. Omtvedt⁷, I. Pysmenetska⁴, D. Renisch³, D. Rudolph⁶, M. Schädel^{4,8}, A. Semchenkov⁷, A. Vascon³, N. Wiehl³, A. Yakushev⁴

¹LBNL, Berkeley, CA, U.S.A., ²U. Liverpool, UK, ³U. Mainz, Germany, ⁴GSI, Darmstadt, Germany, ⁵HIM, Mainz, Germany, ⁶Lund U., Sweden, ⁷U. Oslo, Norway, ⁸JAEA Tokai, Japan

During the $^{244}\text{Pu}(^{48}\text{Ca},3-4n)^{289-288}114$ experiment, high background rates in TASCA were observed and attributed to (i) transfer reaction products (TRPs) that have a magnetic rigidity ($B\rho$) only ~ 15 -30% less than the evaporation residues (EVRs) of interest and decay properties similar to the EVRs and (ii) primary beam passing through pinholes in the target and entering TASCA without charge-exchange or scattering reactions [1]. Both TRPs and primary beam are separated from the evaporation residues (EVRs) of interest in the dipole, but a small fraction are guided back to the focal plane detector by the horizontally focusing quadrupole. This is shown in Fig. 1 for primary beam as compared to EVRs.

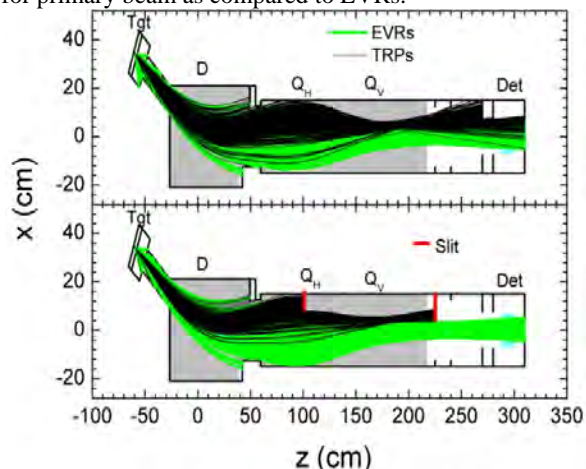


Fig. 1: Primary beam and EVR trajectories in TASCA.

Simulations [2] showed that separation between EVRs and background occurs at the center of the first quadrupole (Q1) and at the exit of TASCA. The use of strategic slits to reduce the acceptance of TASCA in these two areas was expected to result in significantly reduced background without large losses in EVR transmission efficiency as shown in the bottom of Fig. 1. Two solutions (hereafter referred to as M1 and M2) for reducing background in TASCA are:

M1. Introduction of a slit at the center of Q1 reaching from the low $B\rho$ side of TASCA to 8 cm from center. This was expected to result in reductions of 4, 90 and 98% for EVRs, TRPs and primary beam.

M2. M1 plus a slit at the exit of TASCA reaching from the low $B\rho$ side of TASCA to 3.5 cm from center. This was expected to result in reductions of 5, 97 and 99% for EVRs, TRPs and primary beam.

In April 2011, M1 and M2 were tested using the $^{208}\text{Pb}(^{40}\text{Ar},xn)$ reaction, chosen to represent ‘fast’ recoils where the $B\rho$ of the EVRs is approximately 15-30% higher than the $B\rho$ of the TRPs or primary beam. This is similar to what would be expected in reactions such as those currently being investigated to produce elements 119 and 120: $^{249}\text{Bk}(^{50}\text{Ti},xn)$ and $^{249}\text{Cf}(^{50}\text{Ti},xn)$ and the TASISpec element 115 X-ray Fingerprinting experiment.

The high and low energy spectra during the macropulse and the low energy spectra outside of the macropulse for unmodified TASCA, and TASCA with M1 and M2 are shown in Fig. 2. Background reductions of 77 and 84% for TRPs and primary beam, respectively, were observed with M1. For M2, reductions of 93 and 96% were observed for TRPs and primary beam, respectively, in fair agreement with the simulations. Rates of all events in the macropulse were reduced 65 and 88% for M1 and M2, respectively, while the outside of macropulse event rate for M1 and M2 was reduced by 75 and 89%, respectively. The experimental change in EVR transmission efficiency could not be quantified due to the low $^{208}\text{Pb}(^{40}\text{Ar},xn)$ cross section and interference from TRPs.

Without modification, the rate of events in the focal plane detector during the $^{208}\text{Pb}(^{40}\text{Ar},xn)$ reaction was 2900 Hz during the macropulse and 40 Hz outside of the macropulse. With the addition of either M1 or M2, these rates were reduced to <200 Hz inside and <3 Hz outside of the macropulse.

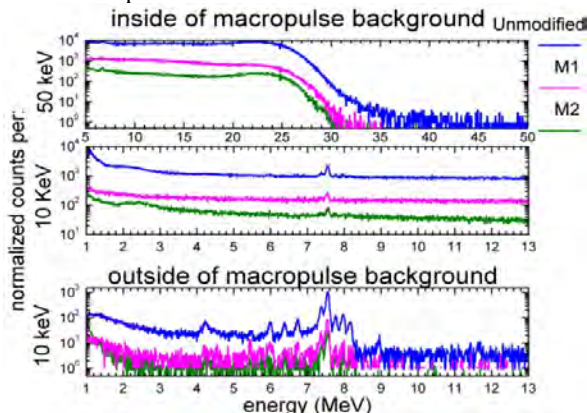


Fig. 2: Total energy spectra for TASCA unmodified and after M1-M2, normalized to the beam integral.

References:

- [1] J.M. Gates *et al.*, Phys. Rev. C **83**, 054618 (2011)
- [2] K.E. Gregorich *et al.*, Phys. Rev. C **71**, 014605 (2005)

IRiS - Feasibility Calculations

J. Dvorak¹ and Ch.E. Düllmann^{1,2,3}

¹Helmholtz Institut Mainz, Mainz, Germany; ²Univ. Mainz, Mainz, Germany; ³GSI Darmstadt, Germany.

The design for a new Inelastic Reactions Isotope Separator (IRiS) [1] to be installed at the GSI Darmstadt has been developed in a joint effort of an international collaboration, headed by the University Mainz, the Helmholtz Institute Mainz, and the GSI. This separator will be dedicated to the investigation of neutron-rich isotopes of heavy and superheavy elements, which can be produced exclusively in multi-nucleon transfer reactions. So far, experimental studies of transfer products with recoil separators have focused on light isotopes not far from stability for a number of reasons. These include low efficiencies for multi-nucleon transfer reactions of recoil separators that are optimized for fusion-evaporation reactions. Here, we present developments toward a dedicated facility featuring an extra-large angular acceptance separator IRiS, which will make the study of heavy neutron-rich transfer reaction products feasible.

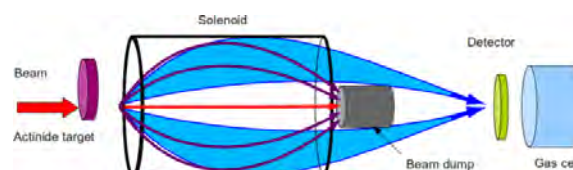
The task of IRiS is to separate reaction products of interest from the primary beam and unwanted byproducts. The separated products will be delivered either into a detector setup or alternatively to auxiliary setups for identification and further investigation of the species of interest. For internal detection in a Si stop detector, maximum acceptable count rates are on the order of 1 kHz. For detection in auxiliary systems like a gas stopping chamber for coupling to external experimental setups, count rates up to 100 kHz appear acceptable.

In our feasibility calculations, two particular nuclear reactions were studied in detail: the reaction $^{48}\text{Ca} + ^{248}\text{Cm}$ at a center-of-mass beam energy $E_{\text{CM}} = 209$ MeV, and the reaction $^{238}\text{U} + ^{248}\text{Cm}$ at $E_{\text{CM}} = 750$ MeV. Predictions for the multi-nucleon transfer channels from theoretical models of V. Zagrebaev [2] and G. Adamian and N. Antonenko [3] were used for these studies. An ion-optical simulation was developed in framework of this study to test the performance of various potential IRiS setups for the two selected reactions. Besides the heavy n-rich products of interest, other reaction byproducts were simulated as well as they will be the major source of background.

Due to large differences in the properties (e.g., velocity, energy, angular emittance) of the studied heavy transfer products when produced in different reactions, the optimal setup differs for either of the reactions. The most versatile setup was found to be one based on a superconducting solenoid magnet as the main component, with a stored energy of $E \sim 10$ MJ. In the simulations, a solenoid magnet with a maximum magnetic field strength of $B_{\text{max}}=4.3$ T and dimensions of 2 m length and 90 cm inner diameter was used. The target is located on axis at the entrance of the solenoid. A beam dump blocking central ions is placed axially at the exit of the solenoid and the detector is located further downstream from the solenoid, see Fig. 1. Ion-optical simulations of the identified opti-

mal setups resulted in efficiencies of roughly 20% for separation of the heaviest ($Z \geq 102$) transfer products, while keeping the background rate well below 100 kHz. For the reaction $^{238}\text{U} + ^{248}\text{Cm}$, the background is predicted to be below 1 kHz, when using a $500\text{-}\mu\text{g}/\text{cm}^2$ thick target. Using thicker targets resulted in increased background. For the reaction $^{48}\text{Ca} + ^{248}\text{Cm}$ two setups were investigated. The setup tuned for detection of the heaviest ($Z \geq 102$) transfer products resulted in background below 1 kHz and the possibility to roughly identify A and Z of the ions. When the setup was adjusted for the detection of Fm isotopes, the background increased to ~ 10 kHz.

Figure 1: Schematic drawing of a solenoid-based IRiS



design in an asymmetric mode. A thin actinide target is bombarded with a heavy-ion beam. A beam dump located on axis behind the solenoid stops both, beam ions, which pass through the target without undergoing nuclear reactions (red arrow) as well as light products of transfer reaction channels (violet). Heavy transfer reaction products (blue) are focused on a disk-like detector at the exit of the solenoid. In the separator mode, the detector is removed, and the products pass through a thin window into the gas-filled stopping cell, where they are available for transport to ancillary setups.

We conclude that the optimal identified setups perform better than expected for the reactions of choice. These setups will most probably not only allow for delivery of separated products into a gas stopping cell, which is the main design requirement, but also enable on-line detection in internal Si detectors. The above described setups offer enough space for inserting of multiple gas-filled detectors for precise TOF measurement and ideally also for a rough Z identification.

Acknowledgment: We thank V. Zagrebaev, G. Adamian and N. Antonenko for sharing results with us prior to publication. Work supported by the Helmholtz Institute Mainz.

References

- [1] J. Dvorak et al., Nucl. Instrum. Meth. A 652 (2011) 687.
- [2] priv. comm.
- [3] priv. comm.

Theoretical Predictions of Properties of Element 119 and its Adsorption* on Noble Metal Surfaces

V. Pershina¹, A. Borschevsky² and J. Anton³

¹GSI, Darmstadt, Germany; ²A. Borschevsky, Massey University, Auckland, New Zealand; ³Institut für Elektrochemie, Universität Ulm, Germany.

In the present work, we predict chemical properties and adsorption behaviour of element 119 that might be produced in the near future at the GSI, Darmstadt. The most promising nuclear reaction appears to be $^{50}\text{Ti} + ^{249}\text{Bk}$, giving the $^{295}119$ and $^{296}119$ isotopes in the $4n$ and $3n$ evaporation channel, respectively. Expected lifetime, of the order of ms, is too short for study of chemical properties of this element using current gas-phase chromatography techniques. However, development of vacuum chromatography could open new prospects in this field.

An analysis of atomic properties, calculated within the Dirac-Coulomb-Breit and other relativistic approaches [1,2] has shown that the relativistic stabilization and contraction of the valence ns AO in group 1 results in the inversion of trends beyond Cs, so that element 119 will be more electronegative than K.

Chemical reactivity of element 119 in comparison with its lighter homologs K through Fr was studied for the M_2 and MAu dimers. Knowledge of properties of these compounds is indispensable for estimating important quantities measured in the chromatography studies, i.e., sublimation, ΔH_{sub} , and adsorption enthalpies, ΔH_{ads} , on gold.

Molecular calculations were performed with the use of our fully relativistic, 4-component, Density Functional Theory method in the non-collinear spin-polarized approximation [3]. Results are given in Tables 1 and 2.

Table 1. Spectroscopic properties of M_2 (M = K through element 119): bond lengths, R_e (in Å), dissociation energies, D_e (in eV) and vibrational frequencies, ω_e (in cm^{-1})^a

Mol.	R_e	D_e	ω_e
K_2	3.942	0.515	91
	<i>3.924</i>	<i>0.520</i>	92
Rb_2	4.224	0.475	58
	<i>4.180</i>	<i>0.485</i>	58
Cs_2	4.673	0.428	41
	<i>4.646</i>	<i>0.452</i>	42
Fr_2	4.610	0.436	33
$(119)_2$	4.265	0.553	41

^a Values in italics are experiment.

The data show that molecular properties have also a reversal of trends beyond Cs. Thus, $(119)_2$ should be most strongly bound in the row of homologs, due to the 8s(119) AO contraction, while 119Au - most weakly, due to the 8s(119) AO stabilization. ΔH_{sub} of the 119 metal and $\Delta H_{\text{ads}}(119)$ on gold were obtained via a correlation with the binding energies of the corresponding dimers in the

* Work supported by HI Mainz

group. Accordingly, $\Delta H_{\text{sub}}(119)$ should be larger than that of K, while $-\Delta H_{\text{ads}}(119)$ on Au (also on Pt and Ag) should be the smallest among the homologs.

Table 2. Properties of MAu (M = K through element 119): bond lengths, R_e (in Å), dissociation energies, D_e (in eV) and vibrational frequencies, ω_e (in cm^{-1})^a

Mol.	R_e	D_e	ω_e
KAu	2.856	2.76	173
	-	2.75	-
RbAu	2.967	2.74	122
	-	2.48	-
CsAu	3.050	2.91	100
	-	2.53	-
FrAu	3.097	2.75	89
119Au	3.074	2.44	92

^a Values in italics are experiment.

Predicted trends in the adsorption of group-1 elements on noble metals are shown in Fig 1. The moderate values of $\Delta H_{\text{ads}}(119)$ are indicative of the feasibility of the chromatography chemical studies.

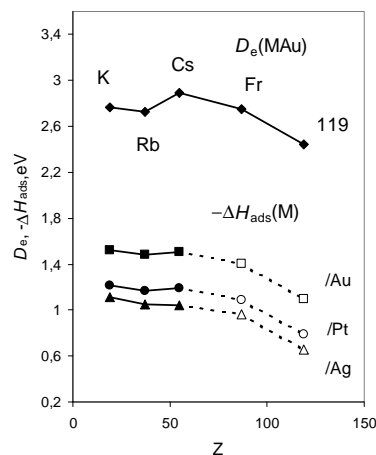


Fig. 1. Calculated $D_e(\text{MAu})$ and $-\Delta H_{\text{ads}}(\text{M})$, where M = K through element 119, on Au, Pt and Ag. (The filled symbols are calculations [4], while open ones – present data).

References

- [1] E. Eliav, *et al.* Chem. Phys. **311** (2005) 163.
- [2] I. S. Lim, *et al.* J. Chem. Phys. **122** (2005) 194103.
- [3] J. Anton, *et al.* Phys. Rev. A **69** (2004) 012505.
- [4] H. Rossbach and B. Eichler, Akademie der Wissenschaft der DDR, Report ZFK-527 (1984).

Prediction of Atomic Properties of Ra and Element 120*

A. Borschevsky^{1,2}, V. Pershina², E. Eliav³, and U. Kaldor³

¹Massey University, Auckland, New Zealand; ²GSI, Darmstadt, Germany; ³Tel Aviv University, Israel

We performed relativistic benchmark calculations of polarizabilities, α , and ionization potentials, IP, of element 120 and its lighter homologues, Ba and Ra. Besides being of fundamental importance in the context of atomic studies of heavy and superheavy elements, these properties are also important for the production and identification of element 120 attempted last year at GSI, Darmstadt [1].

The first and second IPs were calculated using the Dirac-Coulomb-Breit (DCB) Hamiltonian,

$$H_{\text{DCB}} = \sum_i h_D(i) + \sum_{i<j} (1/r_{ij} + B_{ij}).$$

Here, h_D is the one electron Dirac Hamiltonian,

$$h_D(i) = c\boldsymbol{\alpha}_i \cdot \mathbf{p}_i + c^2\beta_i + V_{\text{nuc}}(i),$$

where α and β are the four dimensional Dirac matrices. The nuclear potential V_{nuc} takes into account the finite size of the nucleus, modelled by a uniformly charged sphere. The two-electron term includes the nonrelativistic electron repulsion and the frequency independent Breit operator, B_{ij} , and is correct to the second order in the fine structure constant α .

Correlation was taken into account by the Fock space coupled cluster method (FSCC), augmented by the intermediate Hamiltonian approach [2] to facilitate convergence. The universal basis set [3] was used for both elements. The intermediate Hamiltonian approach allowed us to increase the model space to contain $8s6p6d5f2g1h$ orbitals for Ra, and $8s6p5d4f3g2h$ orbitals for element 120. In order to correct the IPs for higher order QED effects, we used Ref. [4] and added the self-energy, the vacuum polarization, and the frequency dependent Breit energy contributions obtained there on top of our calculated result. The composite effect of the three QED terms lowers the IP of Ra by 46.2 cm^{-1} , and that of element 120 by 101.7 cm^{-1} . The final IPs are shown in Table I in comparison with experiment for Ra and with other calculations for both atoms. The results for Ra are in excellent agreement with the experiment, achieving meV accuracy for the first IP. Similar accuracy is expected for the IPs of element 120, which are higher than those of its lighter homologue due to the relativistic stabilization of the valence ns orbital.

DC calculations of α were performed using the DIRAC08 package [5], employing the finite field approach. Static α of Ra has not been experimentally measured. Thus, along with α of Ra and element 120, we calculated that of their lighter homologue, Ba, for which an experimental value is known [6]. The uncontracted Faegri basis set [7] was used for both atoms and extended to convergence with respect to the calculated polarizabilities. Elec-

* Work supported by HI Mainz and the Marsden Fund, administered by the Royal Society of New Zealand

tron correlation was taken into account at the relativistic CC level, including single, double, and perturbative triple excitations (CCSD(T)). The α s are presented in Table I. To the best of our knowledge, this is the first calculation of α of element 120. The reliability of our prediction is confirmed by good agreement of the obtained α of Ba and Ra with previous calculations and, in case of Ba, with experiment. The decrease in α with increase in atomic number is due to the strong relativistic contraction of the ns orbital.

Table 1. First and second ionization potentials, IP (in eV), and polarizabilities, α (in a.u.), of Ba, Ra, and element 120

Property	Value	Method	Ref
Ba			
α	272.8	DC+CCSD(T)	this
	273.5	DC+CI+MBPT	[8]
	268.2	DC+CCS	[9]
	268±22	exp.	[6]
Ra			
IP1	5.277	DCB+FSCC	this
	5.278	exp.	[10]
IP2	10.176	DCB+FSCC	
	10.147	exp.	[10]
α	242.8	DC+CCSD(T)	this
	248.6	DK+CCSD(T)	[7]
120			
IP1	5.834	DCB+FSCC	this
	5.863	DC+CI+MBPT	[12]
IP2	11.139	DCB+FSCC	this
	11.150	DC+CI+MBPT	[13]
α	167.4	DC+CCSD(T)	this

References

- [1] D. E. Düllmann, *et al.* GSI Annual Report 2011, this issue; S. Hofmann, *et al.* *ibid.*
- [2] E. Eliav *et al.*, J. Chem. Phys. **122**, 224113 (2005)
- [3] G. L. Malli *et al.*, Phys. Rev. A **47**, 143 (1993)
- [4] C. Thierfelder and P. Schwerdtfeger, Phys. Rev. A **82**, 062503 (2010)
- [5] DIRAC08, written by H. J. Ja. Jensen *et al.* (2008)
- [6] H. L. Schwartz *et al.*, Phys. Rev. A **10**, 1924 (1974)
- [7] K. Faegri, Theor. Chim. Acta **105**, 252 (2001)
- [8] S.G. Porsev and A. Derevianko, JETP **102**, 195 (2006)
- [9] B. Sahoo and B. Das, Phys. Rev. A **77**, 062516 (2008)
- [10] C.E. Moore, *Atomic Energy Levels* (U.S. Government Printing Office, Washington, DC, 1958 (1958))
- [11] I.S. Lim *et al.*, Phys. Rev. A **70**, 062501 (2004)
- [12] T. H. Dinh *et al.*, Phys. Rev. A **78**, 022507 (2008)
- [13] T. H. Dinh *et al.*, Phys. Rev. A **78**, 054501 (2008)

Theoretical Studies on Formation and Adsorption of MBr_5 and $MOBr_3$ ($M = Nb, Ta, \text{ and } Db$) on KCl/KBr Surfaces

J. Anton¹ and V. Pershina²

¹Institut für Elektrochemie, Universität Ulm, Germany; ²GSI, Darmstadt, Germany.

Volatility of halides and oxyhalides of the group-5 elements Nb, Ta and Db was studied extensively in the past both experimentally [1-3] and theoretically [4]. The case of adsorption of pure halides revealed some surprises. Thus, theoretical predictions based on the relativistic DS-DV calculations of the electronic density distribution in MBr_5 indicated higher volatility of $DbBr_5$ (as a vapour pressure over the solid) than their lighter homologs in the chemical groups [4], while experimentally, the following trend was observed: $Nb \approx Ta > Db$ [1-3]. New experiments are under way at the IMP, Langzhou, to shed more light on this interesting case [5].

In order to understand adsorption of bromides in these experiments, new theoretical studies were undertaken by us on the basis of the state of art fully relativistic Density Functional Theory (DFT) calculations of various halides, oxyhalides and complexes of the group-5 elements. Our 4 component DFT spin-polarized non-collinear method [6] allows for very accurate calculations of geometrical configurations and stabilities of the heavy-element species. With its use, formation enthalpies and their trend were predicted for the pure pentabromides and oxybromides according to the following reaction



Table 1 contains calculated geometries of the group-5 species of interest together with experimental data where available. Atomization energies are given in Table 2.

Table 1. Bond lengths, R_{ax}/R_{eq} (in Å) in MBr_5 , $MOBr_3$, MBr_6^- , and MBr_5Cl^- and $\angle O-M-Br$ (in degrees) in $MOBr_3$

Molec.	Nb	Ta	Db
MBr_5	2.500/2.449	2.495/2.444	2.548/2.496
	-	2.473/2.412 ^a	-
$MOBr_3$	1.704/2.442	1.716/2.440	1.788/2.484
	1.694/2.429 ^a	-	-
	107.5(107.3 ^a)	104.5	106.0
MBr_6^-	2.554	2.547	2.598
MBr_5Cl^-	2.550/2.380	2.548/2.360	2.600/2.420

^a Experimental values

Table 2. Atomization energies of $MOBr_3$ and MBr_5 (eV)

Molec.	Nb	Ta	Db
$MOBr_3$	20.53	21.43	20.36
MBr_5	18.32	19.41	18.86

It was shown that Db has no preference to bind oxygen, so that the trend in the $MOBr_3$ formation is $Db < Nb < Ta$, in difference to the earlier work [4], while the trend in the MBr_5 formation is $Nb < Db < Ta$. Thus, in the atmosphere

of HBr/BBr_3 , pure pentabromides should be formed. Their volatility as adsorption on an inert surface should have the following trend $Nb < Ta < Db$, in agreement with the earlier conclusions [4]. This trend is, however, not the one observed in the "one-atom-at-a-time" experiments [1-3,5], where the quartz surface is modified (e.g., with aerosol particles KCl , or KBr). Our calculations have shown that on the KBr/KCl surface, the MBr_6^- or MBr_5Cl^- complexes are formed, as is shown in Fig. 1.

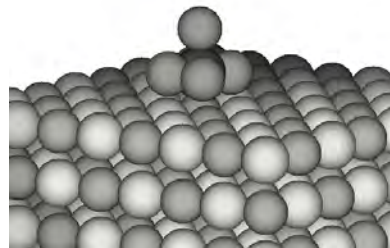


Fig. 1. Formation of MBr_6^- on the KBr surface.

Their geometries are given in Table 1. Complex formation energies with respect to those of Nb, in comparison with the experimental ΔH_{ads} [2,3,5] are given in Table 3.

Table 3. Energies of the $MBr_5 \rightarrow MBr_5L^-$ ($L = Br$ and Cl) reactions, ΔE , and of experimental ΔH_{ads} (in eV), with respect to those of Nb

$-\Delta H_{ads}$	$NbBr_5$	$TaBr_5$	$DbBr_5$
$\Delta E(MBr_5 \rightarrow MBr_6^-)$	0	-0.09	-0.21
$\Delta E(MBr_5 \rightarrow MBr_5Cl^-)$	0	-0.09	-0.25
$-\Delta H_{ads}[SiO_2/KCl]^a$	0	-0.08	-0.29
$-\Delta H_{ads}[SiO_2/KBr]^b$	0	-0.08	-

^a Refs. [2,3]; ^b Ref. [5].

The obtained ΔE (Table 3) are in excellent agreement with the experimental ΔH_{ads} [2,3,5]. Obviously, the complex formation, indeed, takes place on the KCl/KBr surface, so that the trend in the volatility should be $Nb > Ta > Db$.

References

- [1] I. Zvara, *et al.* Sov. Radiochem. **18** (1976) 371.
- [2] H. W. Gäggeler, *et al.* Radiochim. Acta **57** (1992) 93.
- [3] A. Türler, *et al.* Radiochim. Acta **73** (1996) 55.
- [4] V. Pershina, *et al.* J. Chem. Phys. **98** (1992) 1116.
- [5] Qin Zhi, *et al.* Radiochim. Acta, submitted.
- [6] J. Anton, *et al.* Phys. Rev. A **69** (2004) 012505.